



Studies of defects in photonic materials

G.O. Amolo^a, J.D. Comins^{a,b,*}, R.M. Erasmus^{a,b}, T.E. Derry^c

^a Materials Physics Research Institute, School of Physics, University of the Witwatersrand, Johannesburg, Wits 2050, South Africa

^b Raman and Luminescence Laboratory, University of the Witwatersrand, Johannesburg, Wits 2050, South Africa

^c Ion Implantation and Surface Physics Research Programme, School of Physics, University of the Witwatersrand, Johannesburg, Wits 2050, South Africa

ARTICLE INFO

PACS:

61.80.Jh
61.82.–d
61.72.Ji
78.30.–j

Keywords:

Radiation damage
Defects
Proton bombardment
Indium tin oxide
CsI scintillator

ABSTRACT

Indium tin oxide (ITO) films have high optical transmission and infrared reflectance, good electrical conductivity, excellent substrate adherence, hardness and chemical inertness. These properties lead to many applications in the area of photonics. Bombardment of ITO films with 1 MeV protons has been carried out resulting in an observed darkening. Insights into the darkening mechanism that consists of three growth stages as a function of fluence are provided by a study of the optical absorption and X-ray lattice parameter. A new interpretation is provided for the darkening mechanism in terms of the production of defect clusters resulting from the atomic displacements during implantation.

CsI crystals are very effective scintillator materials for particle detectors in high energy physics. Although radiation hard, radiation damage produces colour centres in CsI that reduce light emission and can negatively affect the luminescent centres. Using a combination of Raman and optical absorption spectroscopy applied to CsI crystals bombarded with 1 MeV protons at 300 K, the resulting defects are shown to be *F*-type centres and interstitial *V*-centres having the I_3^- structure and being responsible for absorption bands at 2.7 and 3.4 eV. Isochronal and isothermal annealing experiments show a mutual decay of the *F* and *V*-centres. The results are discussed in relation to the formation of interstitial iodine aggregates of various types in alkali iodides.

© 2009 Elsevier B.V. All rights reserved.

1. Introduction

Photonic materials are of major importance in many branches of science and engineering. The present work reviews progress in understanding the role of radiation induced defects in two such materials, namely indium tin oxide (ITO) and caesium iodide (CsI) that have specialist applications.

Indium oxide I_2O_3 when doped with Sn forms the material indium tin oxide (ITO) [1]. Applications include coatings on solar collectors, energy-efficient windows on buildings, flat panel display electrodes and transparent conducting electrodes on solar cells [2]. An ITO sample for solar energy applications has a transmittance of ~80% in the visible region of the spectrum being characterised by two transmittance limits, the interband transitions at short wavelengths and at long wavelength by the concentration of free carriers. Ion bombardment of ITO films has been shown to result in darkening accompanied by increases in resistivity, but the mechanism responsible has not been previously identified. ITO is radiation hard at low fluences with little

darkening, but at high fluences the darkening is more rapid [3,4]. The present work reviews new insights into the darkening mechanism in terms of the development of defect clusters [5].

The mechanism of irradiation damage and the resulting defects in alkali halide crystals have been subject to a large number of studies; these have been restricted in the main to compounds having the f.c.c. NaCl structure [6,7]. The simple cubic (s.c.) alkali halides have been rather neglected in this context, but relatively recently pure CsI has received increased interest, mainly as a result of its success as a fast scintillator in electromagnetic calorimeters for high energy physics experiments [8–13]. CsI has the advantage having high efficiency and high density leading to a small radiation length as well as being radiation hard, even in the high radiation environments encountered. Indeed, early work indicated extreme resistance to defect production by X- and ^{60}Co γ -ray irradiation [14,15] and success was only achieved in later work with high radiation flux γ -ray doses [16] and high energy charged ions [9,11,12].

The spectra and decay times of the 4.3 and 3.7 eV luminescence bands associated with the self-trapped excitons (STE's) have been studied by Nishimura et al. [17]. They depict the on-centre and off-centre configurations of the STE's in the s.c. structure that are analogues of those in f.c.c. structured alkali halides. These suggest that the radiation damage process would be excitonic in nature and that the primary defects would be *F* centres and *H*

* Corresponding author at: Materials Physics Research Institute, School of Physics, University of the Witwatersrand, Johannesburg, Wits 2050, South Africa. Tel.: +27 11 717 6812; fax: +27 11 717 6879.

E-mail address: darrell.comins@wits.ac.za (J.D. Comins).

centres. In spite of the practical usefulness of CsI, and the appreciation that the defects produced in sufficiently high radiation environments negatively affect the luminescent centres and reduce light emission [12], in depth studies of their structures have been limited, in most cases being restricted to the measurement of *F* centres. The present work reviews new information on the production and annealing of both halogen vacancy and halogen interstitial defects in CsI [18] of relevance to its applications as a scintillator. The techniques involve a combination of Raman and optical absorption spectroscopy which have proved most successful in studies of the radiation induced defects in the f.c.c. alkali iodides [19–24].

2. Experimental

2.1. Indium tin oxide (ITO)

ITO films having a thickness of 610 nm were prepared from a target with composition 10 wt% SnO₂ and 90 wt% I₂O₃ and deposited on 2 mm thick float glass substrates. The samples were bombarded with 1 MeV protons within the fluence range 1×10^{15} – 250×10^{15} cm⁻² near room temperature (RT) and 373 K, respectively. Optical transmission and absorption measurements were made at RT after the proton bombardments and at chosen intervals thereafter. The optical absorption of the glass substrate was essentially unchanged after proton bombardment.

Complementary X-ray diffraction studies were performed on the samples irradiated at RT. The four main diffraction peaks from the planes (2 2 2), (4 0 0), (4 4 0) and (6 2 2) of the I₂O₃ lattice were studied.

2.2. Caesium iodide (CsI)

Randomly oriented samples of approximate dimensions $8 \times 8 \times 2.5$ mm³ were cut from a nominally pure CsI crystal boule and surfaces mechanically polished to a finish of 1 μm. They were bombarded by 1 MeV protons at 300 K, care being taken to minimise beam heating effects, and subsequently stored under high purity argon gas at a temperature below 273 K.

The irradiated samples were mounted in a micro-cryostat permitting optical absorption and Raman measurements. The optical absorption studies were carried out at either 80 or 300 K. Raman measurements were performed at 77 K with a low laser beam power of 1.5 mW on the sample to avoid optical bleaching of the colour centres.

Optical absorption and Raman spectroscopy were used to study the effects of isochronal and isothermal annealing of the irradiated samples. The results were analysed by the procedures of Ref. [23] to determine the reaction order and activation energy.

3. Results and discussion

3.1. Indium tin oxide (ITO)

SRIM2003 simulations of the electronic and nuclear energy loss, ion range distribution and the vacancy concentrations for the proton bombardment were carried out for ITO. Owing to their limited thickness, the protons pass through the ITO films and are brought to rest within the float glass substrates. While the electronic stopping is dominant, and nuclear stopping is very small throughout the films, at the higher fluences there will be substantial vacancy concentrations created by nuclear collisions. The resulting defects are likely to contribute significantly to the overall optical effects observed.

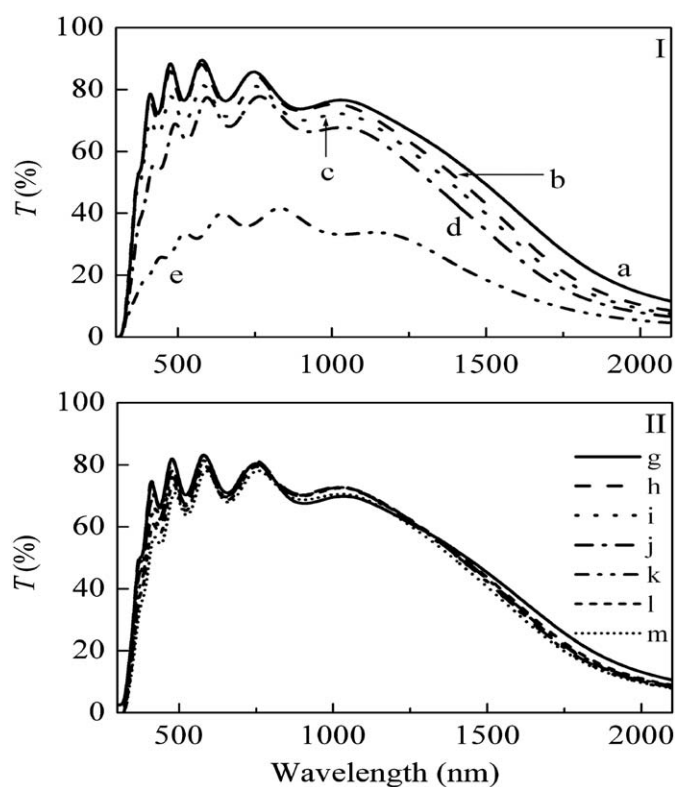


Fig. 1. Transmission spectra of selected ITO samples as a function of wavelength resulting from 1 MeV proton bombardment with increasing fluence. I shows results for RT irradiations (a: unirradiated; b: 1×10^{15} ; c: 6×10^{15} ; d: 40×10^{15} ; e: 250×10^{15} ions/cm²). II shows results for irradiations at 373 K (g: unirradiated; h: 6×10^{15} ; i: 40×10^{15} ; j: 120×10^{15} ; k: 190×10^{15} ; l: 215×10^{15} ; m: 250×10^{15} ions/cm²).

Fig. 1 shows the changes in the optical transmission of the ITO films over a wide wavelength range as a function of 1 MeV proton fluence at RT (I) and 373 K (II). By comparison of the spectra of the unirradiated samples of ITO with the simulated spectra of Hamberg and Grandqvist [2] the free electron density of the present samples is estimated to be 8×10^{20} cm⁻³.

In the case of the RT bombarded samples, the transmittance reduces with increasing fluence over a broad range of wavelengths. A near 40% decrease in transmittance has occurred at the highest fluence of 250×10^{15} ions/cm² corresponding to obvious darkening of the sample. For the 373 K bombardment there are only small decreases in the transmission even for the highest fluence.

Following storage of the irradiated ITO films for a month at RT there were only small changes in transmission for samples irradiated within the fluence range 1 – 40×10^{15} cm⁻² but a significant recovery for the sample bombarded with fluence 250×10^{15} cm⁻².

Complementary X-ray diffraction studies over the same fluence range were performed on the samples immediately after irradiation at RT and a month later. Examination of the four main diffraction peaks of the I₂O₃ lattice from the planes (2 2 2), (4 0 0), (4 4 0) and (6 2 2) confirmed that the crystalline structure of I₂O₃ was preserved. The lower fluence samples had essentially similar X-ray diffraction patterns as the unirradiated sample, but at the highest fluences namely 40×10^{15} and 250×10^{15} cm⁻², small decreases in the peak angles and increases in the *d*-spacings occurred. In the case of the highest fluence sample there was a significant reduction in the X-ray diffraction peak intensity. After storage at RT for one month, this sample displayed a recovery of

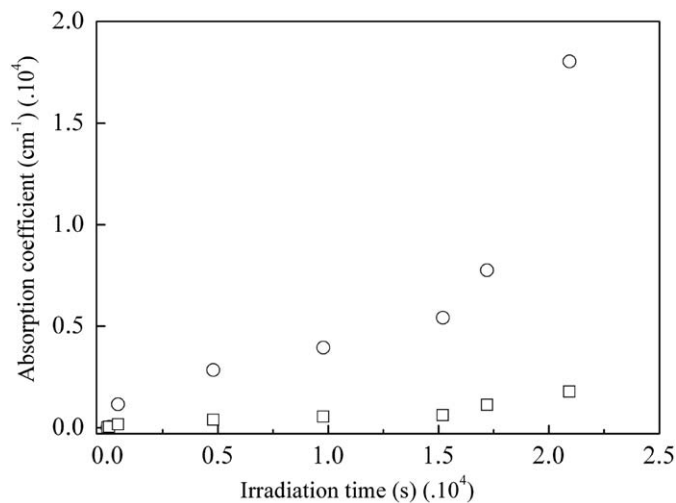


Fig. 2. The variation of the absorption coefficient at 550 nm with irradiation time for two similar samples of ITO films. Circles: irradiation at RT; squares: irradiation at 373 K.

the peak angles and d -spacings close to their original values and a substantial recovery of the peak intensity.

Fig. 2 shows the increase in optical absorption and hence film darkening resulting from the proton bombardments at RT and 373 K. A three-stage growth of absorption as a function of irradiation time is observed at both RT and 373 K. Rapid initial growth is observed during the first stage. In the second stage slowly increasing absorption occurs which evolves into more rapid growth within the third stage. Similar features are displayed during the irradiation at 373 K, but the growth of absorption is much slower especially in the second and third stages.

The three stage behaviour is modelled using a system of coupled differential equations adapted from earlier work on the creation of defect clusters in irradiated alkali halides [25,26]. It is assumed that complementary defects are produced by a primary mechanism, one of which is stable and the other mobile. Clusters are formed of the mobile defects by heterogeneous nucleation by pre-existing defects or impurities. Detrapping is considered to occur from an intermediate small aggregate, while the ultimate large clusters are stable. Temperature dependent rate constants are included in the trapping and detrapping terms [25]. The equations were solved numerically with appropriate initial conditions, leading to the simulated growth curves shown in Fig. 3. There is good qualitative agreement with the experimental results in regard to the three stages of defect growth and their respective temperature dependence.

Further support for the concept of defect clusters being responsible for the darkening of ITO is provided by the variation of the irradiation-induced change in absorbance A with wavelength λ for the various proton fluences used. This relationship is found to be $A \propto 1/\lambda$ in the case of the highest fluence irradiation of 250×10^{15} ions/cm² being in agreement with the predictions of the Mie theory [27] in the limit of small spherical absorbing particles of radius $R \ll \lambda$.

It is thus concluded that the darkening mechanism in 1 MeV proton bombarded ITO results from the production of lattice displacements ultimately leading to the formation of absorbing defect clusters. A kinetic model of defect production involving heterogeneous trapping of mobile defects at pre-existing imperfections and detrapping from intermediate dimeric clusters, successfully describes the defect growth process and its temperature dependence. X-ray diffraction investigations are consistent with the conclusions of the optical studies. A full account of this

work, including the kinetic model of defect production will appear elsewhere [28].

3.2. Caesium iodide (CsI)

The optical absorption spectra of CsI as a function of 1 MeV proton fluence are shown in Fig. 4. The spectra show the presence of the F and F_2 bands at 1.68 and 1.1 eV, [14,15], the latter being considerably more intense than the former. The most prominent features in the ultraviolet part of the spectrum conventionally known as the V band region are at 2.7, 3.4 and 4.2 eV, the first two being broad bands. The sharp 4.2 eV band, and its smaller satellites at 4.05 and 4.35 eV differ greatly in appearance from the broad bands. The growth curves of the most prominent bands

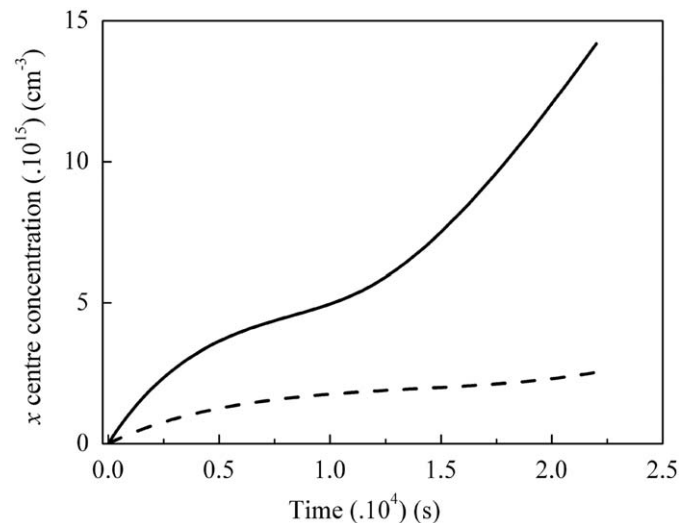


Fig. 3. Simulation of the variation of the defect concentration of the immobile x centres with irradiation time at different temperatures. Solid line: irradiation at RT; broken line: irradiation at 373 K.

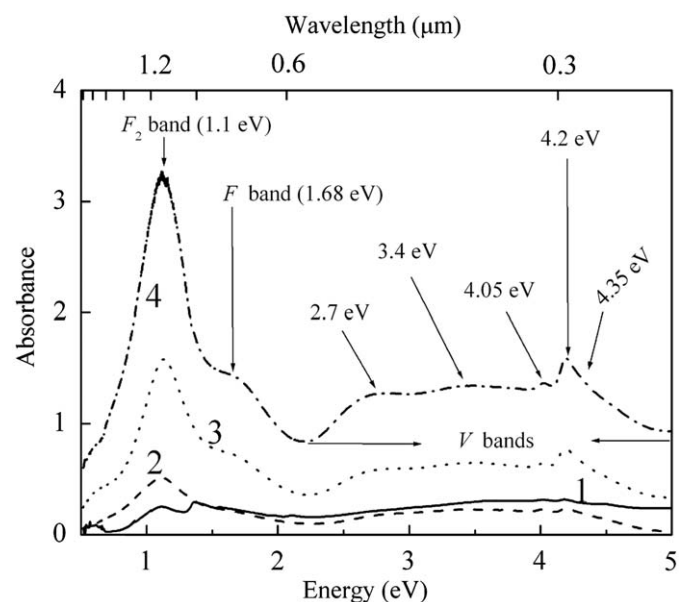


Fig. 4. Development of optical absorption features in proton bombarded CsI with increasing fluence at 300 K (1: 5×10^{15} ; 2: 1×10^{16} ; 3: 3×10^{16} ; 4: 6×10^{16} ions/cm²). Optical measurements were performed at RT.

F_2 , 2.7, 3.4 and 4.2 eV bands show a near linear relationship as illustrated in Fig. 5.

Fig. 6a illustrates the Raman spectrum of CsI resulting from 1 MeV proton bombardment with a fluence of 6×10^{16} ions/cm² at a temperature of 300 K. A strong fundamental Raman peak at 113 cm^{-1} is present together with a series of seven overtones.

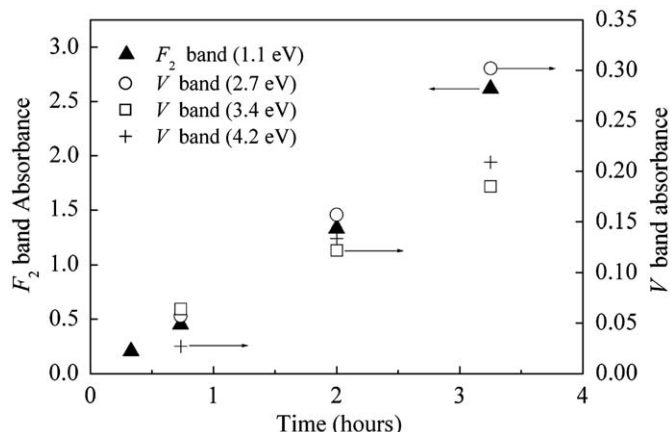


Fig. 5. Growth of the F_2 band at 1.1 eV and the V bands at 2.7, 3.4 and 4.2 eV as a function of time of bombardment with 1 MeV protons at 300 K.

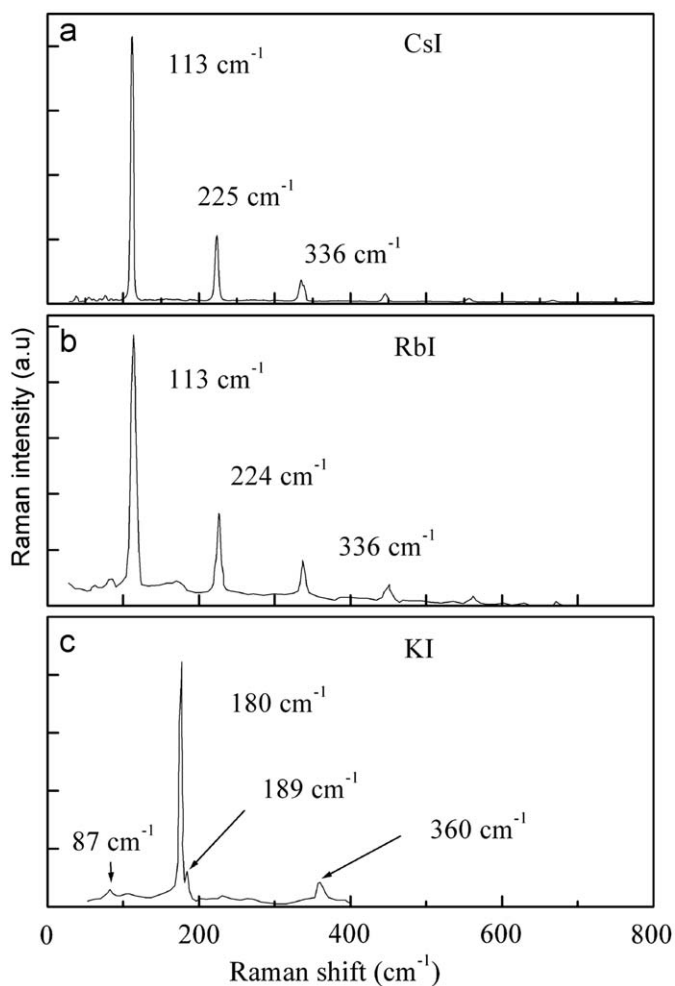


Fig. 6. Raman spectra of: (a) The 1 MeV proton bombarded CsI at 300 K; (b) γ -irradiated RbI at 295 K; (c) X-irradiated KI at 295 K.

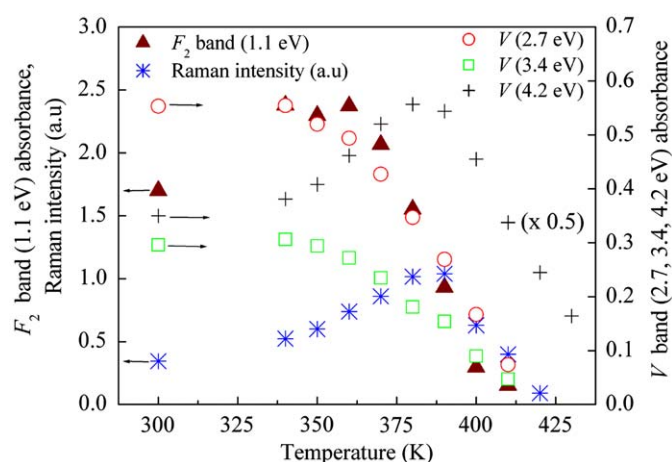


Fig. 7. Results of the isochronal annealing of the CsI sample. The decay of the concentration of the respective defects as a function of temperature during the anneal is determined by optical absorption for the F and V bands and Raman spectroscopy for the I_3^- aggregates.

These Raman features are characteristic of dimeric I_3^- clusters [19–21].

The isochronal annealing behaviour of the various optical absorption features and the complementary behaviour of the 113 cm^{-1} Raman feature were investigated for the sample bombarded with a proton fluence of 6×10^{16} ions/cm² and are shown in Fig. 7. There is a major annealing stage at $\sim 385 \text{ K}$, involving the mutual decay of the F_2 band, the V bands at 2.7 and 3.4 eV and the Raman features at 113 cm^{-1} with its series of overtones. The 4.2 eV band decays at a higher temperature of $\sim 410 \text{ K}$.

Isothermal annealing at a temperature of 397 K near the midpoint of the major annealing stage as determined by the isochronal anneal was performed on a further sample also receiving a proton fluence of 6×10^{16} ions/cm². Again there is good correlation between the decay of the F_2 band, the V bands peaking at 2.7 and 3.4 eV and the 113 cm^{-1} Raman peak.

In the analysis of the annealing processes, the chemical rate equations of Ref. [23] are used. As shown in Fig. 8a, by using the isothermal annealing results, the reaction is shown to be of second order. Using the isochronal annealing results and the appropriate relation for a second order reaction, the activation energy is determined as $E = 1.28 \text{ eV}$ as shown in Fig. 8(b).

The annealing experiments demonstrate that the F -type centres and the dimeric I_3^- clusters responsible for the broad V bands at 2.7 and 3.4 eV are complements. The sharp bands near 4.2 eV are considered to be impurity related.

In assessing the results on CsI it is necessary to compare them with complementary experiments on the f.c.c. alkali iodides. It is noted that for irradiations near RT, the Raman results for CsI are rather similar to those of RbI [23], namely that the dimeric I_3^- clusters are the dominant interstitial halogen defects. This is also the case for KI irradiated at temperatures near 200 K [22]. Since the dimeric I_3^- clusters are the lowest order H centre aggregates, this strongly supports the idea that the primary defects in CsI namely F and H centres are created by an excitonic mechanism similar to those in the f.c.c. alkali halides, but with an altered geometry corresponding to the s.c. lattice and the configurations of the self-trapped excitons [17]. Thus the marked radiation hardness of CsI, so vital in its application as a scintillator in high radiation environments could at least in part be the result of the inefficiency of the excitonic mechanism in creating the primary defects. This awaits theoretical investigations similar to those on the f.c.c. alkali halides [6,7] that would develop an understanding

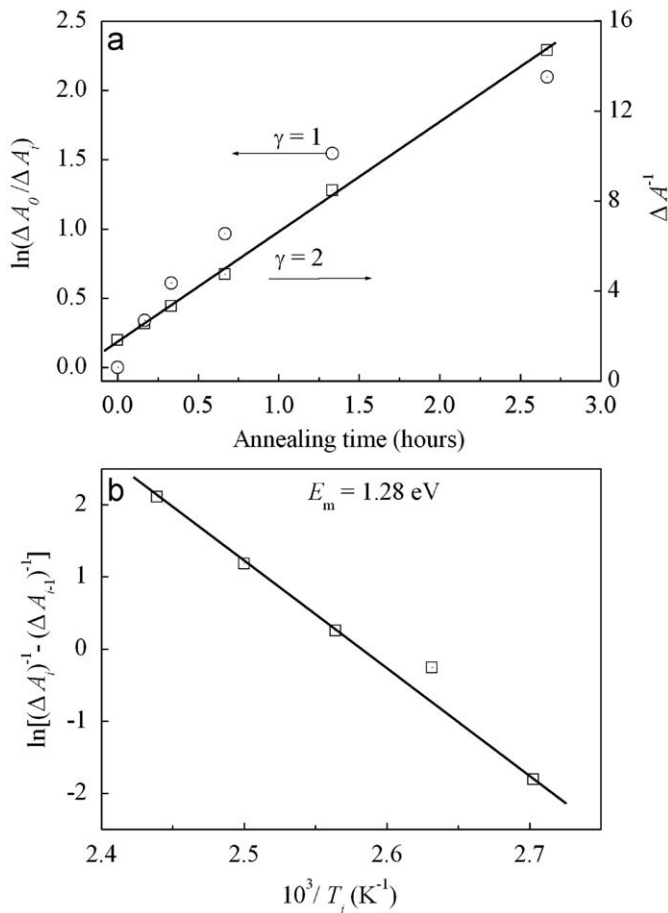


Fig. 8. (a) Determination of the reaction order for vacancy-interstitial recombination using the results of isothermal annealing of the F_2 band at 397 K. From the equations of Ref. [23], a plot of $\ln(\Delta A_0/\Delta A_t)$ vs. total annealing time t yields a straight line for a first-order reaction ($\gamma=1$), whereas a plot of ΔA^{-1} vs. t yields a straight line for a second-order reaction ($\gamma=2$). The results show that the reaction is second order. (b) Determination of the activation energy of the vacancy-interstitial recombination from the isochronal annealing of the F_2 band. The plot of $\ln[(\Delta A_t)^{-1} - (\Delta A_{t-1})^{-1}]$ vs. $10^3/T_i$, as discussed in Ref. [23], yields a straight line for the present case of $\gamma=2$ from which the activation energy of 1.28 eV is obtained for the reaction.

of the apparent threshold of electronic excitation needed for defect production, as well as the geometry of the F - H pair and its separation.

A second aspect in considering the radiation hardness of CsI is to consider the progression of relative cation size of the alkali iodides. While irradiations near RT for RbI and CsI result in the formation of dimeric I_2^- clusters as the dominant interstitial halogen defects as discussed above, these results are in stark contrast to those for KI irradiated at RT whose Raman spectrum, shown in Fig. 6c, contains an intense doublet at 180 and 189 cm^{-1} resulting from large $(I_2)_n$ molecular iodine aggregates [19–22]. The V band in KI is broad and lacks the structure present for those in RbI and CsI. The annealing kinetics, corresponding to interstitial-vacancy recombination, are second order for RbI [23] and CsI, being consistent with separated point defects but first order for KI in which the interstitial aggregates are large clusters [29]. The formation of the latter is a thermally activated process, indicated by the increasing proportion of these in the defect inventory as the temperature of irradiation is raised [22].

In the f.c.c. alkali iodides the relatively small cation K leads to the large $(I_2)_n$ aggregates being formed in irradiated KI near room temperature while under similar conditions the relatively larger

cation Rb results in the formation of the small clusters I_3^- in RbI. The yet larger cation Cs in s.c. CsI also results in these small clusters. In terms of a current model of the formation of F and V centres under irradiation and their relationship to the formation of perfect dislocation loops, observed in the electron microscope [30], cation displacements are also necessary in addition to the anion displacements originated by the excitonic mechanism. The vacancy pairs thus formed are able to provide sites for the small interstitial clusters such as I_3^- . An extension of this process can therefore provide the necessary void space for large clusters, provided that the cations can be displaced. Smaller cations such as K would be relatively more easily displaced, particularly once sufficiently high temperatures are attained. The large Cs cation would be the most difficult to displace leading to radiation hardness.

4. Summary

Two examples have been selected to demonstrate the effects of defects on the characteristic and useful properties of two very different photonic materials, namely ITO and CsI. In each case the respective studies have provided new insights into the defect structures and their formation.

In the case of ITO thin films that have several photonic applications, the favourable optical transparency is diminished by 1 MeV proton bombardment. This leads to the formation of absorbing defect clusters whose presence provide a self consistent explanation of the optical darkening, the defect growth kinetics and the lattice changes observed by X-ray diffraction.

For the radiation hard scintillator CsI the investigations provide an in-depth study of the structures of the defects formed, their production and high temperature annealing behaviour. Mechanisms leading to the radiation hardness are examined.

Acknowledgements

This material is based on work supported by the National Research Foundation under Grant number 2053306. The authors are grateful for the research support of the University of the Witwatersrand. We thank iThemba Labs (Gauteng) for the use of the proton accelerator facility.

References

- [1] J.H.W. de Wit, J. Phys. Chem. Solids 20 (1977) 143.
- [2] I. Hamberg, C.G. Granqvist, J. Appl. Phys. 60 (1986) R123.
- [3] D.V. Morgan, A. Salehi, Y.H. Aliyu, R.W. Bunce, D. Diskett, Thin Solid Films 258 (1995) 283.
- [4] T.J. Vink, H.F. Overwijk, W. Walrave, J. Appl. Phys. 80 (1996) 3734.
- [5] J.D. Comins, G.O. Amolo, T.E. Derry, S.H. Connell, R.M. Erasmus, M.J. Witcomb, Nucl. Instrum. and Meth. B 267 (2009) 2690.
- [6] K.S. Song, R.T. Williams, Self trapped excitons, in: M. Cardona (Ed.), Springer Series in Solid State Physics, Springer-Verlag, Berlin, 1993.
- [7] N. Itoh, A.M. Stoneham, Materials Modification by Electronic Excitation, Cambridge University Press, Cambridge, UK, 2001.
- [8] S. Kubota, S. Sakuragi, S. Hashimoto, J. Ruan, Nucl. Instrum. and Meth. A 268 (1998) 275.
- [9] M. Kobayashi, M. Ieiri, K. Kondo, T. Miura, H. Noumi, M. Numajiri, Y. Oki, T. Suzuki, M. Takasaki, K. Tanaka, Y. Yamanoi, Nucl. Instrum. and Meth. A 328 (1993) 501.
- [10] C.L. Woody, P.W. Levy, J.A. Kierstead, T. Skwarnicki, Z. Sobolewski, M. Goldberg, H. Horwitz, P. Souder, D.F. Anderson, IEEE Trans. Nucl. Sci. 37 (1990) 492.
- [11] Z. Wei, R. Zhu, Nucl. Instrum. and Meth. A 326 (1993) 508.
- [12] A.I. Popov, E. Balazat, Nucl. Instrum. and Meth. B 166–167 (2000) 545.
- [13] K. Suzuli, H. Fujimura, R. Hashimoto, T. Ishikawa, J. Kasagi, S. Kuwasaki, K. Mochizuki, K. Nawa, Y. Okada, Y. Onodera, M. Sato, H. Shimizu, H. Yamazaki, A. Kawano, Y. Sakamoto, K. Maeda, Modern Phys. Letters 24 (2009) 978.
- [14] P. Avakian, Phys. Rev. 120 (1960) 2007.
- [15] D.W. Lynch, A.D. Brothers, D.A. Robinson, Phys. Rev. 139 (1965) A285.

- [16] S. Lefrant, E. Rzepka, *J. Physique Coll.* 41 (1980) C6–C476.
- [17] H. Nishimura, M. Sakata, T. Tsujimoto, M. Nakayama, *Phys. Rev. B* 51 (1995) 2167.
- [18] G.O. Amolo, R.M. Erasmus, J.D. Comins, T.E. Derry, *Nucl. Instrum. and Meth.* 250 (2006) 359.
- [19] S. Lefrant, E. Rzepka, *J. Phys. C: Solid State Phys.* 12 (1979) L573.
- [20] E. Rzepka, S. Lefrant, L. Taurel, A.E. Hughes, *J. Phys. C: Solid State Phys.* 4 (1981) L767.
- [21] A.M.T. Allen, J.D. Comins, P.J. Ford, *J. Phys. C: Solid State Phys.* 18 (1985) 5783.
- [22] A.M.T. Allen, J.D. Comins *Nucl. Instr. and Meth. B* 65 (1992) 516.
- [23] A.M.T. Allen, J.D. Comins, *J. Phys. Condens. Matter.* 4 (1992) 2701.
- [24] M.A. Pariselle, S. Lefrant, E. Balanzat, B. Ramstein, J.D. Comins, *Phys. Rev. B* 53 (1996) 11365.
- [25] J.D. Comins, B. Carragher, *Phys. Rev. B* 24 (1981) 283.
- [26] M. Aguilar, F. Jaque, F. Agullo-Lopez, *Radiat. Effects* 61 (1982) 215.
- [27] H.C. van de Hulst, *Light Scattering by Small Particles*, Wiley, New York, 1957.
- [28] G.O. Amolo, J.D. Comins, T.E. Derry, to be submitted for publication (2009).
- [29] A.M.T. Allen, J.D. Comins, *Crystal Lattice Defects and Amorph. Mat.* (1987) 93.
- [30] L.W. Hobbs, A.E. Hughes, D. Pooley, *Proc. Roy. Soc. A* 332 (1973) 167.